Adhesion of *Aureobasidium pullulans* Is Controlled by Uronic Acid Based Polymers and Pullulan

Jill M. Pouliot, Ian Walton, Matthew Nolen-Parkhouse, Laila I. Abu-Lail, and Terri A. Camesano*

Department of Chemical Engineering, Worcester Polytechnic Institute, Worcester, Massachusetts 01609

Received November 6, 2004; Revised Manuscript Received December 22, 2004

Aureobasidium pullulans is a potentially pathogenic microfungus that produces and secretes the polysaccharide pullulan and other biomacromolecules, depending on the microbe's physiological state. The role of these macromolecules in mediating adhesion and attachment were examined. Interfacial forces and adhesion affinities of *A. pullulans* were probed for early-exponential phase (EEP) and late-exponential phase (LEP) cells, using atomic force microscopy (AFM). Biochemical assays showed that *A. pullulans* produces both pullulan and a uronic acid based polymer. The pullulan is not produced until the LEP, and it can be removed by treatment with pullulanase. Both adhesion forces between the microbe and the AFM tip (silicon nitride) and attachment of the cells to quartz sand grains were controlled by the density of the uronic acid polymer. Uronic acid polymers doubled in density between the EEP and the LEP and were unaffected by the enzyme pullulanase. Retention to quartz in a packed column was quantified using the collision efficiency (α), the fraction of collisions between the microbes, and the sand grains, that result in attachment. Adhesion forces and retention on glass were well correlated, with these values being higher for EEP cells ($F_{adh} = 7.65 \pm 4.67$ nN; $\alpha = 1.15$) than LEP ($F_{adh} = 2.94 \pm 0.75$; $\alpha = 0.49$) and LEP + pullulanase cells ($F_{adh} = 2.33 \pm 2.01$ nN; $\alpha = 0.43$). Steric interactions alone do not describe the adhesion behavior of this fungus, but they do provide information regarding the length and density of the macromolecules studied.

Introduction

Aureobasidium pullulans is a microfungus (micron-sized fungus) found in soil and water, especially upon decaying leaf litter, wood, and other plant life.[1] It is frequently categorized as a mild plant pathogen, particularly for grapes, and plays a vital role in the post-harvest decay of many crops. *A. pullulans* is also an opportunistic human pathogen, especially in immuno-compromised hosts. Infections can range from subcutaneous to deep tissue,[2] and serious infections have been noted such as in the spleen[3] and in the serous membrane of the abdominal cavity.[4]

A. pullulans produces and secretes pullulan, a high molecular weight polysaccharide that consists of repeating units of maltotriose connected by α-(1→6)-glycosidic links, with a lesser number of maltotetraose units. The pullulan produced by this microbe is usually black pigmented, caused by melanin contamination. The virulence of *A. pullulans* is in part controlled by the pigmented melanin in the cell wall, which provides the microbe resistance to phagocytosis in the host.[2] However, naturally occurring and mutant strains of *A. pullulans* exist that produce reduced levels of melanin.[5,6]

A. pullulans may produce other macromolecules, depending on culture conditions. For example, cells grown on sucrose produce pullulan and an acidic glucan with uronic acid components, whereas cells cultured on maltose produce a heteropolysaccharide containing glucose, galactose, and mannose.[7] Besides pullulan, *A. pullulans* cells can produce an acidic heteropolysaccharide (glucose, galactose, mannose, and glucuronic acid) and a β-linked glucan when grown in xylose.[8] Production can be modified for optimization of a certain component, often pullulan. For example, Gibson and Coughlin demonstrated that the highest yield of pullulan (and least amount of melanin) could be obtained by growing strain NRRL Y-2311-1 on sucrose in a fermentor agitated by marine propellers, compared to 4 alternate strains and other forms of agitation.[9]

Biosynthesis of pullulan and the other macromolecules by *A. pullulans* has been studied, but conflicting results appear in the literature as to where the pullulan is located and the mechanisms of assembly and secretion. From an analysis of the literature, it seems likely that the pullulan is present external to the cell wall, since it is a nonstructural polysaccharide. Discrepancies were noted regarding the need for a cell wall in pullulan production. Catley and Hutchison demonstrated that a plasma membrane and an intact cell wall were necessary for the production of pullulan, since treatment with Zymolase (a wall-lytic compound) impaired pullulan synthesis.[10] One study claimed cell-free synthesis of pullulan,[11] but this was not reproducible in later attempts.[12,13]

The function of pullulan is related to the location and assembly. Although fungal cells often produce polysaccharide for the purpose of energy storage, this does not appear to be the function of pullulan in *A. pullulans*, since the microbe cannot break the polysaccharide down to easily metabolized sugars.[1] While pullulan is most likely not a

* To whom correspondence should be addressed. Telephone: 508-831-5380. Fax: 508-831-5853. E-mail: terric@wpi.edu.

10.1021/bm0492935 CCC: $30.25
Published on Web 01/22/2005

storage material, it is believed to serve for cell protection and to aid in adhesion of *A. pullulans* to surfaces in the environment,[1] such as leaf surfaces[14] or wood.[15]

If the adhesion of *A. pullulans* is believed to be governed by polymer production, and this production depends on growth phase, then it is logical to assume that the physiological state of the organism would impact its adhesive properties. Some studies have suggested that pullulan is expressed more in later growth stages because it is a secondary metabolite. Therefore, it can be produced more when growth becomes limited or as the cells approach stationary phase.[1]

Molecules additional to pullulan that are also produced by this fungus have received even less study. Use of molecular-level tools, such as the AFM, represents a powerful approach to directly probe and quantify microbial interactions and to study fungal macromolecules.[16−18] The AFM also allows the complex problem of the role of physiological status on bioadhesion to be probed. In this study, we investigated the role of physiological status on the interaction forces and adhesion of *A. pullulans* and related nanoscopic properties of the fungal biopolymers, as measured with the AFM, to the attachment of the fungi to a model surface (quartz sand).

Materials and Methods

Microbial Growth. *A. pullulans* strain NRRL Y-2331-1, which produces high yields of a nonpigmented form of pullulan,[9] was obtained from the United States Department of Agriculture (USDA). The growth media consisted of a complex nitrogen stock solution with sucrose as the carbon source,[5] containing (per 1 L of ultrapure water): 2.0 g of yeast extract, 0.5 g of $(NH_4)_2SO_4$, 1.0 g of NaCl, 0.2 g of $MgSO_4$, 3.0 g of K_2HPO_4, 0.01 g of $FeSO_4$, 0.01 g of $MnSO_4$, 0.01 g of $ZnSO_4$, and 50 g of sucrose. All ingredients, excluding $ZnSO_4$, $MnSO_4$, $FeSO_4$, and $MgSO_4$, were mixed and autoclaved for 45 min at 121 °C. For the remaining metals, stock solutions were prepared and sterile-filtered using 0.45-μm syringe filters, to avoid possible precipitation of the metals during autoclaving.

A. pullulans was maintained in frozen micro-centrifuge tubes containing 1 mL of cells grown in the nitrogen/sucrose media. A thawed tube was added to 5 mL of fresh nitrogen/sucrose media and placed on a tube rotator for 18−24 h. From this preculture, 1 mL of inoculum was added to 50 mL of fresh nitrogen/sucrose media and agitated at ∼200 rpm. A growth curve was difficult to obtain since the culture is yeast-like during exponential growth but becomes mycelial in stationary phase. The optical density of the suspension was measured hourly at a wavelength of 600 nm using a spectrophotometer (Thermo Spectronic, Genesys 20). However, once cells were approaching the stationary phase, we were unable to obtain accurate data due to cell aggregation and immobilization on the glass vessel. We therefore concentrated our experiments on two time points within exponential growth, labeled for our convenience as "early-exponential phase" (EEP) and "late-exponential phase" (LEP), corresponding to 3 and 6 h of growth.

A sample of LEP cells was treated with the enzyme pullulanase, produced by *Bacillus acidopullulyticus* (Sigma). This enzyme hydrolyzes the α-(1→6) linkages of pullulan, which are the dominant type of linkages present. All cultures of *A. pullulans* were harvested by centrifugation (6000 rpm, 1000 × g, 25 °C, 15 min for all centrifugation steps) and washed twice with 20 mM MES buffer (pH = 6.4). For the enzyme-treated cells, washed cells in MES buffer were incubated with pullulanase (0.1 mg/mL) for 60 min at 100 rpm and at 40 °C. After treatment, cells were centrifuged, washed in MES buffer once, then centrifuged, and resuspended in ultrapure water (Millipore milli-Q water). All microbial experiments were performed in ultrapure water, but we caution that the behavior of the microbes at higher ionic strengths has not been tested.

Cell sizes and counts were determined by staining cells with acridine orange, a dye that is fluorescent when viewed with an epifluorescent microscope (Eclipse 3100, Nikon). Cells were stained and viewed on a black membrane filter (Millipore) at 1000×, using a published procedure.[19]

Exopolymer Collection. Since pullulan is produced and secreted extracellularly by *A. pullulans*, it is not necessary to fractionate the cell wall to collect exopolymers. Extracellular material was separated from the cell suspension by centrifugation for 30 min at 10 000 × g (25 °C). Biomass was quantified following the procedure reported by Lee et al.,[20] in which cells were washed with ultrapure water and dried at 100 °C until the weight remained constant. Crude products were precipitated from the supernatant by dissolving the exopolymer in 2 volumes of ethanol (95%) and incubating at 4 °C for 24 h. This material was washed repeatedly in acetone and ether, and following several exchanges, the material was lyophilized, following a published protocol.[20]

Biochemical Assays. A colorimetric assay was performed to determine the uronic acid content of the extracellular material for the three tested conditions, following the modified carbazole reaction.[21,22] Sulfamate was added so that neutral sugars would not produce browning.[23] Diphenyl was added to help color the uronic acids at room temperature.[23] Glucuronic acid was used as the calibration standard (125−7500 nmol/mL). The amount of uronic acid present in the samples was normalized to the dry weight of the cells.

The protein content in the extracellular material was assayed using the Lowry technique,[24] with bovine serum albumin as the calibration standard (10−500 ppm).

Cell Immobilization Protocol for AFM Experiments. Fungal cells were attached to clean glass slides for AFM experiments. Slides were soaked in a 3:1 mixture of hydrochloric acid/nitric acid (25 min), followed by a copious rinsing with ultrapure water (Milli-Q, Millipore Corp), soaking in a 4:1 mixture of sulfuric acid/hydrogen peroxide (25 min), and further rinsing with ultrapure water.

A. pullulans cells were attached to clean, amino-silane coated glass slides, as described elsewhere.[25] Briefly, clean glass slides were coated with 3-aminopropyltrimethoxysilane, which imparts an NH_2- functionality to the glass surface. Then, microbes were immobilized using the zero-length cross-linker 1-ethyl-3-(3−dimethylaminopropyl)carbodiimide (EDC), stabilized by sulfo-hydroxysuccinimide (sulfo-NHS),

which formed a link between microbial carboxyl groups and the amino groups on the glass slides. This technique has been successfully used to prepare a variety of microbial cells for AFM force analyses,[25,26] and previous work has shown that these chemicals do not alter cell viability.[27] The zero-length cross-linkers modify amino acid side groups (on the glass slide) to permit cross-link formation, but they do not remain as part of the linkage, nor do they modify the microbial surface. After the bonding reaction, slides were transferred to a Petri dish containing ultrapure water.

Microbial cells were imaged with the AFM (Digital Instruments Dimension 3100 with Nanoscope III controller) in tapping mode under water before performing force analyses. The spring constant of the silicon nitride tips (Digital Instruments; DNPS tips) was measured to be 0.13 $\pm$ 0.02 N/m, using the Cleveland method[28] and the correlation equations given in the Digital Instruments software. Tips were cleaned prior to use by exposure to ozone generated by ultraviolet light irradiation in an oxygen atmosphere for 1 min, which removes any organic carbon contamination covering the tip apex.[29]

For each experimental condition, representative images were captured. A line trace was performed over the microbial surface to characterize the roughness. The roughness was quantified in terms of the peak distance between asperities (λ) and the root-mean square roughness (*rms*). Five cells were examined in each case and the λ and rms values were averaged.

Force Analysis Using AFM. Forces were measured between hydrated individual fungal cells and silicon nitride cantilevers using an AFM. To select a cell for analysis, an image was obtained in tapping mode of a portion of the glass slide. The tip was then positioned over the center of a cell, the rastering of the cantilever was stopped, the tapping was turned off, and a force measurement was performed. At least five measurements were performed on a single area of each microbial cell and such measurements were performed on 4−5 fungal cells for each experimental condition. Force cycles were recorded during the approaches and retractions of the tip with the samples.

The data files were calibrated according to the procedure of Ducker et al., which is valid when the cantilever is a weaker spring compared to the sample.[30] The cantilever deflects linearly with piezo position and the probe makes rigid contact with the sample surface. Since the cantilever is too weak to cause deformation of the sample, cantilever deflection in the "constant compliance" region must be entirely due to the movement of the piezo. Therefore, we can determine the position of the sample surface by aligning the constant compliance region to the force axis. Cantilever deflections could be converted to force values using the measured tip spring constants.

Several other steps were taken to ensure that artifacts were not induced in the force measurements. For example, force measurements made on at least 5 areas over the top of a microbe were captured and determined to be nearly identical (<5% variation). Force measurements were not made at the edges of the cells since this may cause artifacts. In addition, force measurements were made on clean glass before and after force measurements on fungal cells, to ensure that the tip was not contaminated during the course of the experiment.

Steric Repulsion Forces between Cellular Biopolymers and AFM Tip. A model accounting for steric interactions between two interacting surfaces, one covered with grafted polymers and the other bare, was developed by Alexander[31] and de Gennes,[32] and modified by Butt et al.[33] to describe the interactions of an AFM probe with a polymer brush

$$F_{st} = 50 k_B T a L_1 \Gamma_1^{3/2} \exp(-2\pi h/L_1) \quad (1)$$

where, F_{st} is the force due to steric interactions integrated across the surface of the probe (N m^{-2}), k_B is the Boltzmann constant (J K^{-1}), L_1 is the equilibrium polymer brush length (m), h is the distance between the probe and the sample (m), T is the absolute temperature (K), a is the tip radius of curvature (m), and Γ_1 is the grafted polymer density (m^{-2}). Drummond and Senden showed that, although the probe has a nominal radius of curvature of 40 $\pm$ 20 nm,[34,35] its behavior in terms of long-range interaction energies (van der Waals, electrostatic, etc.) is that of a much larger (130−380 nm) sphere. A larger radius of 250 nm was demonstrated to be appropriate for the modeling of steric interactions between a silicon nitride tip and microbial biopolymers.[25]

In some cases, single values of L_1 and Γ could not characterize the observed forces. An extension to the steric model was applied that allowed for two polymer layers with different densities and equilibrium lengths.[36] In eq 1, the term $L_1\Gamma_1^{3/2} \exp(-2\pi h/L_1)$ is replaced, such that

$$F_{st} = 50 k_B T a [L_1 \Gamma_1^{3/2} \exp(-2\pi h/L_1) + L_2 \Gamma_2^{3/2} \exp(-2\pi h/L_2)] \quad (2)$$

where L_1 and Γ_1 refer to the equilibrium length and density of the first brush and L_2 and Γ_2 refer to the equilibrium length and density of the second brush.

Adhesion/Retention Assays of Microbes on Quartz Sand. To eventually relate the results of this study to microbial attachment to environmentally relevant surfaces, the transport of the microbes through packed columns containing quartz media was quantified in terms of the collision efficiency (α), the fraction of striking microbes that attach to the collectors. The porous medium was quartz sand (Sigma), having a diameter of 327 $\pm$ 40 μm (determined by image analysis of 50 particles), and cleaned as described previously.[37]

The glass column (length = 15 cm, diameter = 1.0 cm) was packed with dry silica sand (Sigma) in 1 cm increments using the "tap and fill" method, to ensure that packing was uniform and devoid of air pockets. *A. pullulans* solutions in ultrapure water corresponding to EEP, LEP, and LEP + pullulanase conditions were prepared as described above. Ultrapure water was pumped through the column (0.02 mL/s) using a peristaltic pump for >2 h to ensure that the column was equilibrated. Then, 10 pore volumes (one pore volume ~4.5 mL) of the *A. pullulans* solution were pumped through the column, followed by a 10 pore volume rinse with ultrapure water (0.02 mL/s). During the microbial injection and subsequent rinsing, a fraction collector was used to collect samples of the effluent solution in sterile glass tubes.

The concentration of microbes in the effluent solution at each time point (C) was quantified by measuring the absorbance at 600 nm, and these concentrations were compared to the influent concentration of *A. pullulans* (C_0). A breakthrough curve was constructed of C/C_0 versus time. This cellular transport experiment has been previously shown to yield reproducible results, with maximum differences between individual columns <5%.[38]

The steady-state breakthrough concentration of the microbial cells was used to estimate the collision efficiency (α) for each experiment, using the one-dimensional colloid filtration equation developed by Yao et al.,[39] as

$$\alpha = \frac{-2d_c \ln(C/C_0)}{3(1-\theta)\eta_c L} \quad (3)$$

where C/C_0 represents the "steady-state" breakthrough concentration of microbial cells estimated from the breakthrough curves (C being the number concentration of microbes at any time and C_0 being the number concentration of microbes that were introduced into the column), θ is the porosity of the media (0.40), d_c is the collector diameter (327 μm), and L is the length of the column (15 cm). In the Rajagopalan and Tien model for the collector efficiency, η_c is taken as the sum of the physical forces affecting collisions: diffusion, effects of neighboring particles, London-van der Waals forces, interception, and gravitational settling.[40,41]

Results

Biochemical Assays. The uronic acid contents were 12 ± 0.8, 20.4 ± 2.4, and 20.9 ± 1.7 nmol/mg dry wt. of cells, for EEP, LEP, and LEP + pullulanase cells, respectively. The amount of protein in all of the samples was negligible.

Reproducibility in AFM Measurements during Probe Approach to Microbial Cell Surfaces. In each force measurement, the tip was positioned over the center of the cell and 5 force curve cycles (approach + retraction) were recorded. We examined the data sets from each series of 5 cycles and determined that the approach curves were highly reproducible. Figure 1 shows the reproducibility in the approach curves on a single EEP cell, although similarly reproducible results were seen with LEP cells. For each condition (EEP and LEP cells), we measured at least 5 force cycles on 4−5 individual cells.

Comparison of EEP and LEP Cells in Terms of Interaction Forces. Both EEP and LEP cells showed repulsive interactions during the approach of the AFM probe with the sample, but these repulsions were larger in magnitude and extended over longer distances for LEP cells (Figure 2). The repulsive forces decayed exponentially as a function of distance, and could be well described by the steric model (Table 1). When the force−distance data are plotted as the natural log of the force versus separation distance, a linear relationship should be observed. This was true for EEP cells, and the slopes and intercepts were used to determine the equilibrium polymer brush length to be 39.5 nm (Figure 3A). For LEP cells, this relationship was sometimes observed

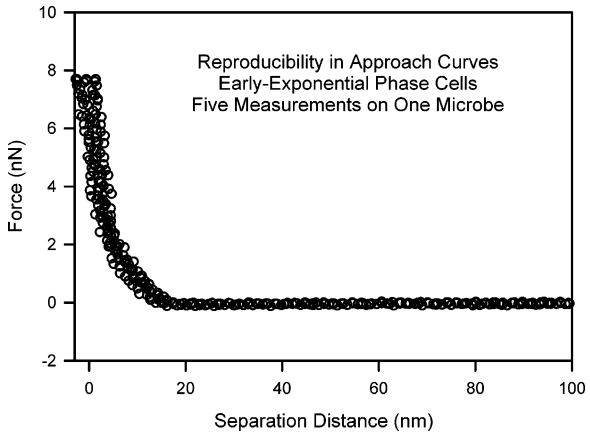

Figure 1. Reproducibility in approach measurements on a single cell. Five measurements were made over the center of one cell, and all data points are shown. The same procedure was used for all cells under all experiments. On a single cell, in approximately the same location, the approach curves are reproducible. The values in the approach curves generally vary by <25%. For example, for the cell shown, the average approach forces at separations of 1, 10, 15, and 20 nm are 6.46 ± 0.86, 0.81 ± 0.18, 0.19 ± 0.05, and 0.07 ± 0.01 nN, respectively.

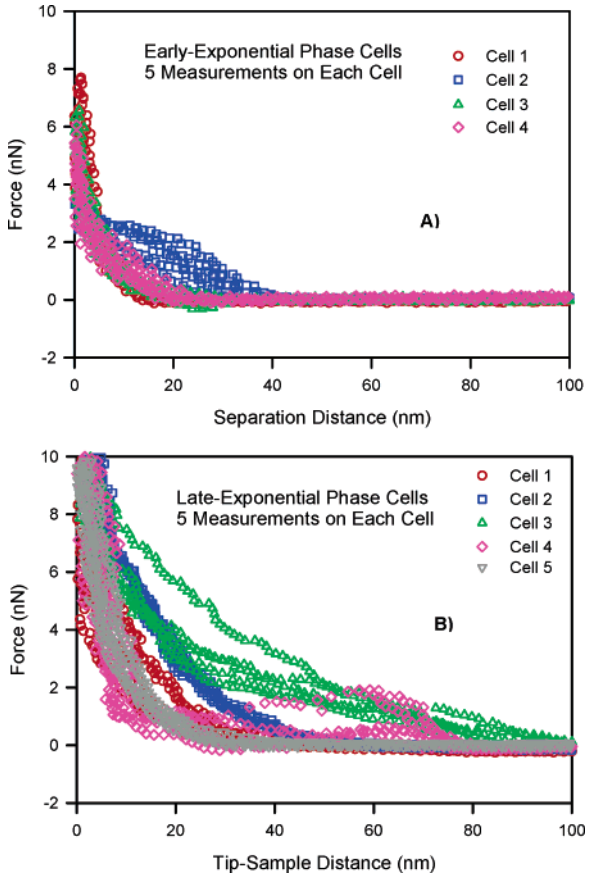

Figure 2. AFM approach curves for *Aureobasidium pullulans*. For each cell shown, 5 measurements were made over the top of that cell (all data is shown, no averaging has been performed). (A) Measurements on EEP cells. (B) Measurements on LEP cells.

(Figure 3B), but in 4 of the 5 cells examined (and for all 5 passes on each of those 4 cells), the plots revealed two regions with distinctly different slopes (Figure 3C). The equilibrium polymer lengths were 34.1 and 80.2 nm, for these two regions, respectively. In addition, the density for the longer brush was nearly an order of magnitude higher than

Table 1. Equilibrium Polymer Length and Density Based on Application of the Steric Model[a]

	L_1 (nm)	L_2 (nm)	Γ_1 (1/nm^2)	Γ_2 (1/nm^2)	R^2 for population 1	R^2 for population 2
EEP cells	39.5	NA	0.0214	NA	0.93	NA
LEP cells	34.1	80.2	0.040	0.379	0.90	0.96
LEP cells + pullulanase	40.7	NA	0.039	NA	0.90	NA

[a] NA indicates that the second population was not observed. For EEP Cells and LEP Cells + pullulanase, eq 1 was used to fit data. For LEP Cells, eq 1 or 2 was used to fit data (see Figure 3 caption).

the density of the shorter brush, suggesting that ~10% of the polymers on LEP cells are of the shorter population (Table 1). Between the EEP and LEP, the density of the shorter polymers almost doubled (increased by 90%).

Pullulanase-Treated LEP Cells. After treatment of LEP cells with the enzyme pullulanase, the AFM force measurements during the approach portions of the cycles again showed repulsion that could be well described by the steric model (Figure 4; Table 1). The pullulanase-treated LEP cells showed only a single population of macromolecules (data not shown), with lengths very close to the lengths of the molecules on EEP cells (40.7 nm versus 39.5 nm). However, the density of these short polymers was increased by 86%. When comparing between LEP and LEP + pullulanase treated cells, we found that the properties of the short population of biopolymers changed very little (L_1 and Γ_1), but the second subpopulation was eliminated by the pullulanase treatment.

Control cells, which were centrifuged but not subjected to enzymatic treatment, behaved identical to the untreated cells (data not shown). This suggests that the centrifugation steps alone did not remove or alter these biopolymers, probably because a very low centrifugal force was used (1000 × g). Research from our laboratory has demonstrated that this low centrifugal force does not change AFM force measurements for other microbes.[42]

Adhesion Forces after Contact between Cellular Polymers and AFM Probe. The retraction cycles of the AFM force curves were examined to gain information regarding the adhesion forces between the sample and the tip after contact. A typical retraction curve may have one or more adhesion peaks (Figure 5). Unlike what we usually observe for bacterial systems (multiple peaks of fairly similar magnitude), these retraction curves typically showed one dominant adhesion peak and sometimes showed one or more much smaller peaks. We compared the magnitude of the maximum adhesion peak for each measurement made, to develop a histogram showing how the polymers are mapped on the cell surface, a technique suggested by Gad et al.[43] This resulted in a total of 20 measurements (4 cells × 5 measurements/cell or 5 cells × 4 measurements/cell) per condition (EEP cells, LEP cells, and LEP cells with pullulanase treatment). The adhesive forces were significantly greater ($P < 0.001$, Mann−Whitney rank sum test) for cells from the EEP compared to the LEP, with averages of 7.65 ± 4.67 and 2.94 ± 0.75 nN for EEP and LEP cells, respectively (Figure 6). Data corresponding to the second peak (when present) are difficult to interpret, especially when the force has not returned to zero after the first peak (cf.

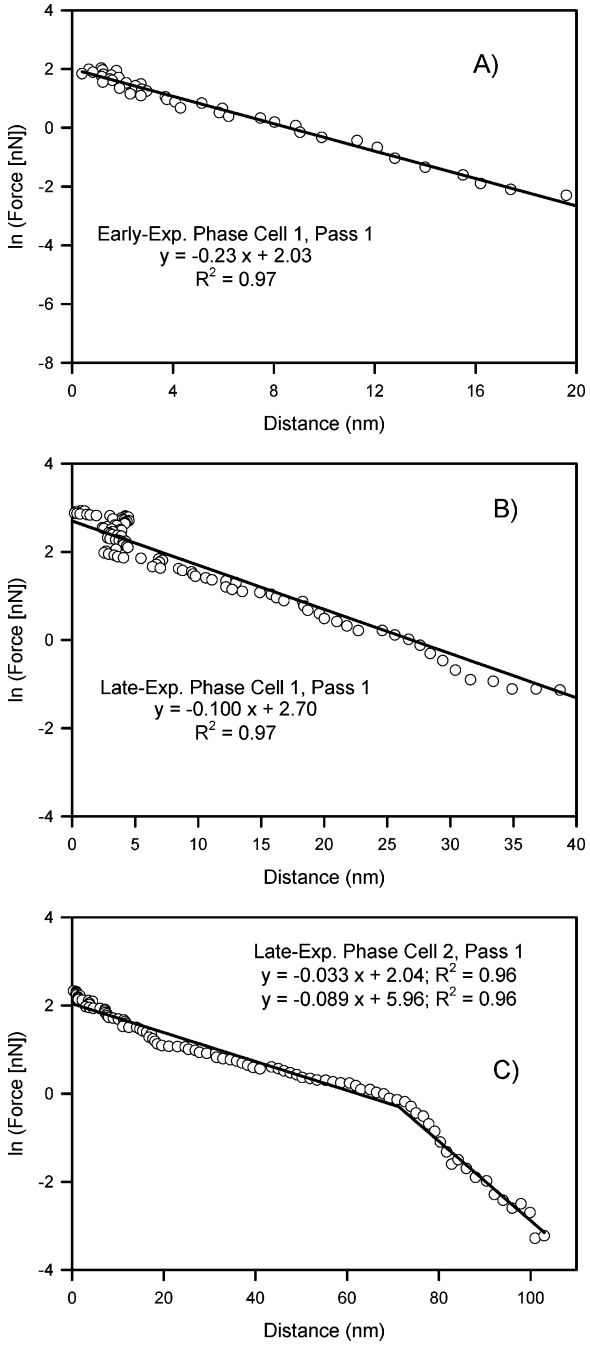

Figure 3. Representative examples of fits with the steric model for approach curves on *A. pullulans*. The natural log of the force (left-hand side of eq 1 or 2) is plotted versus the distance. The slope and the intercept are used to calculate the equilibrium polymer lengths and densities, according to eqs 1 and 2. In general, eq 1 was used when a single polymer length could characterize the data. If this resulted in a poor fit, and the data clearly showed regions with two different slopes, then eq 2 was applied. All of the data for EEP cells and the LEP + pullulanase cells could be characterized by a single population of molecules, and so eq 1 was always applied. The LEP cells contained some data sets that showed 2 polymer populations, and some that showed only 1. In these cases, we attempted to use eq 1, but if the R^2 values were very poor, eq 2 was applied. Six out of 26 data sets showed a single population, with the rest all showing 2 populations of polymers. (A) An example of one pass on an EEP cell; (B) Example of one pass on a LEP cell, in which a single length and grafting density can characterize the polymer behavior; (C) LEP cell exhibiting two subpopulations with different equilibrium lengths and polymer grafting densities. The average equilibrium lengths and grafting densities for all of the cells examined are shown in Table 1.

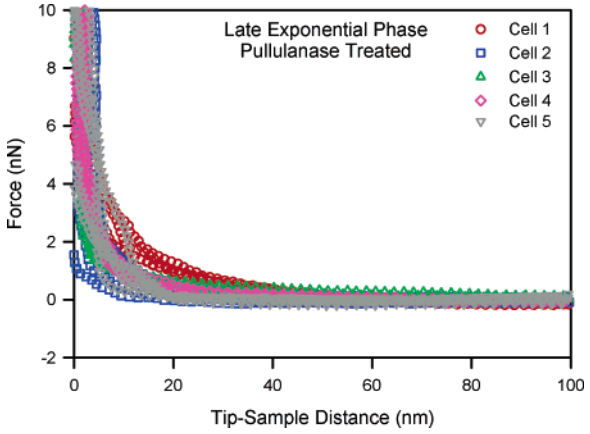

Figure 4. AFM approach curves for *Aureobasidium pullulans* cells treated with the enzyme pullulanase, which hydrolyzes the α-(1→6) linkages.

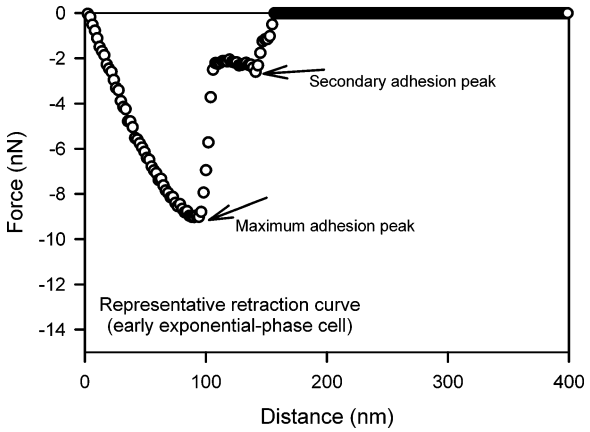

Figure 5. Representative retraction curve shown here for an EEP cell. The maximum adhesion peak was noted in each force measurement.

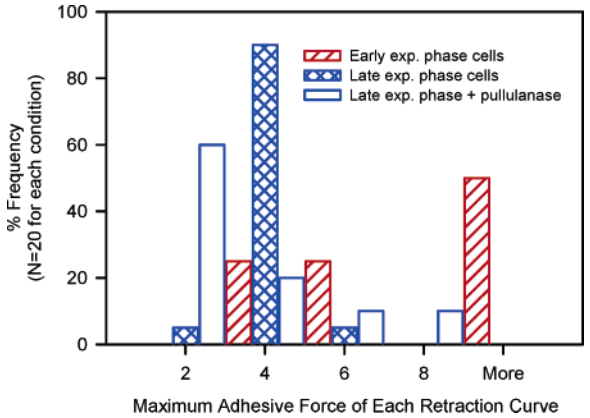

Figure 6. Histogram showing the distribution of adhesion affinities for the three samples studied (EEP cells, LEP cells, and LEP cells that had been treated with pullulanase). For each retraction curve that was analyzed (cf. Figure 5), 1−5 adhesion peaks were observed. In most cases, there was one dominant peak. The maximum force corresponding to the largest adhesion peak was considered, as described in the text. There was no case in which an adhesion peak was not observed. There were a total of 20 maximum adhesion force measurements for each condition studied, corresponding either to 4 cells probed 5 times each (untreated EEP and LEP cells) or 5 cells probed 4 times each (for the pullulanase-treated cells).

Figure 5). We cannot tell if the second peak represents another polymer chain or just an alternate location on the first chain.

Table 2. Correlation between Collision Efficiency and Adhesion Force

conditions	collision efficiency	average adhesion force (nN)
EEP cells	1.15	7.65 ± 4.67
LEP cells	0.49	2.94 ± 0.75
LEP cells + pullulanase	0.43	2.33 ± 2.01

Pullulanase treatment decreased the adhesion affinity between the microbes and the tip, to an average value of 2.33 ± 2.01 nN (Figure 6). The maximum adhesive forces between the polymers on pullulanase-treated cells and untreated cells (EEP or LEP) were statistically different from one another ($P < 0.001$, Mann−Whitney rank sum test).

Cellular Attachment to Quartz. For each experimental condition tested, breakthrough curves were obtained that showed steady-state behavior [data not shown, but similar to other published results, cf. ref 37]. The steady-state C/C_0 value was estimated from the breakthrough curve and used to calculate the α values with eq 3. The collision efficiencies from the packed column experiments were compared for the three experimental conditions, and correlated with the average adhesion forces based on AFM retraction curve data. The collision efficiency of EEP cells was high (1.15; Table 2) and decreased by 57% and 62% for LEP and LEP + pullulanase cells, with values of 0.49 and 0.43, respectively. The high collision efficiency of EEP cells (above a value of one) is sometimes observed in laboratory-scale columns. The high value may be attributable to the difficulty in correctly modeling the number of collisions between the fungal cells and the quartz grains, as collision efficiencies >1 are sometimes calculated using this model.[44] The correlation between the collision efficiency and the average adhesion force between the fungal cell and silicon nitride (from the AFM data) was good. The average adhesion force was 7.65 nN for EEP cells and decreased by 62 and 69% for LEP and LEP + pullulanase cells, respectively (Table 2).

Discussion

Relating Fungal Adhesion and Attachment. The adhesion forces measured via the AFM retraction curves were well correlated with attachment of *A. pullulans* to quartz sand in a packed-column system. The appropriateness of the silicon nitride tip to mimic attachment to quartz media probably is due to the similar physical nature of these surfaces. We previously found that attachment of *Escherichia coli* to quartz was also well correlated with AFM adhesion force measurements with silicon nitride.[37] Energy calculations based on DLVO theory between *E. coli* and either quartz or silicon nitride were identical,[37] due to the fact that both quartz and silicon nitride have zeta potentials of −16 mV under similar conditions[45,46] and that the DLVO interactions were dominated by electrostatic interactions. Although Lifshitz-van der Waals interactions between the bacterial cells and the two surfaces are expected to be different, these interactions were very small compared to the electrostatics.

Modeling Fungal Adhesion. AFM retraction curves exhibited one or more adhesive events between fungal

macromolecules and the silicon nitride tip. Although there is a distribution in the adhesion forces, tests confirmed that there was a statistically significant decrease in adhesion between the EEP cells and either the LEP or LEP + pullulanase cells (Mann−Whitney rank sum test). Further, LEP cells and LEP + pullulanase cells did not show statistically significant differences in the adhesion forces, as the data sets were not different enough to exclude the possibility that variation was caused by chance.

We wanted to determine if the adhesive forces observed were explainable through a model for van der Waals forces, which is given by

$$F_{\text{adh}} = -\frac{A}{6h^2}\left(\frac{a_1 a_2}{a_1 + a_2}\right) \quad (4)$$

where A is the Hamaker constant, h is the separation distance, a_1 is the cell radius, and a_2 is the tip radius. In this case, h is replaced by the distance of closest approach, H_0, usually assumed to be 0.3 nm.[47] This calculation results in a force of 30.9 nN, which is much higher than we observed experimentally in any of the retraction measurements. The discrepancy probably lies in the fact that this model was developed for smooth and uniformly spherical surfaces, unlike the surface of *A. pullulans*.

For consideration of rough surfaces, a different form of the van der Waals expression can be used, in which the roughness of the adhering particle (*A. pullulans* in this case) is accounted for. Strictly speaking, the AFM tip also has a roughness associated with it, but the roughness of silicon nitride is at a smaller scale than the roughness of the microbial cell. If we assume that the roughness in the interaction is primarily due to the distribution of biopolymers and other macromolecules on the microbial surface, then the appropriate model for calculating the adhesion force has been derived by Rabinovich et al. as[47,48]

$$F_{\text{adh,rough}} = -\frac{Aa_2}{6H_0^2}\left[\frac{1}{1 + \left(\frac{32a_2k_1\,\text{rms}}{\lambda^2}\right)} + \frac{1}{\left(1 + \frac{k_1\text{rms}}{H_0}\right)^2}\right] \quad (5)$$

where a_2 is the tip radius, H_0 is the distance of closest separation (0.3 nm), k_1 is a coefficient equal to 1.817, and the terms rms and λ refer to the asperities on the surface. If a line trace is performed on an AFM image of the microbe, the peak distance between asperities is λ, and rms is the root-mean square of the surface roughness.

AFM images on *A. pullulans* revealed that the λ and rms values changed with the physiological state and with pullulanase treatment (Table 3). Using these values allowed us to calculate the van der Waals forces of adhesion based on the "rough" model of Rabinovich et al.[47,48] Adhesion values obtained with said model were qualitatively consistent with the measured values, although their magnitudes were decreased by about half. This factor of 2 between the experimental and model data may reflect the choice of the tip radius for this system.

Even if absolute numbers differ between the experimental and model-predicted values, the rough model still gives a much better agreement than the traditional van der Waals expression and correctly addresses all experimental conditions. The conventional van der Waals model accounts only for the radius of the microbe, which would be nearly unchanged between the two growth phases and would have little dependence on whether enzymatic removal of surface polymers was performed. Therefore, all three types of cells examined would have the same adhesive interaction with silicon nitride, which was clearly not observed experimentally. Also, by using the radius of the whole microbe as the surface for interaction, the forces are over-predicted by 4−13-fold compared to observed values. The combined consideration of van der Waals interactions and surface roughness is able to semiquantitatively characterize the adhesive behavior of *A. pullulans* with silicon nitride at both growth phases and to account for the possibility of treatment with pullulanase. This result suggests that the relatively simple modified van der Waals model (the Rabinovich et al. expression) can be very useful in predicting the adhesion of microbial cells.

Table 3. Absolute Magnitude of Measured and Calculated Adhesion Forces, Using van der Waals Expressions for Smooth and Rough Surfaces

	F_{adh}, measured (nN)	F_{adh},vdW[b] (smooth) (nN)	rms (nm)	λ (nm)	F_{adh},vdW[c] (rough) (nN)
EEP cells	7.65 ± 4.67	30.9	2.3	50	3.75
LEP cells	2.94 ± 0.75	30.9	4.3	44	1.54
LEP cells + pullulanase	2.33 ± 2.01	30.9	18	41	1.22

[a] The Hamaker constant was taken to be 1×10^{-19}J for all three cases. [b] Calculated van der Waals interaction using eq 4 with a closest separation distance of 0.3 nm. [c] Calculated van der Waals interaction using eq 5 with a closest separation distance of 0.3 nm.

Conceptual Model of Polymer Production and Properties for *A. pullulans*. The results of our AFM experiments, transport assays, and biochemical tests allowed us to create a new conceptual model of the behavior of macromolecules associated with *A. pullulans* as a function of physiological status and to relate the properties of these macromolecules to adhesion (Figure 7). To culture pullulan, fermentors are often run for long periods of time to maximize pullulan production, on the order of several days.[9] For the hour 3 cells in our study, we have very little exopolymer, and due to the size (39.5 nm) and chemical information, it is apparently entirely uronic acid based. The size of this polymer is sufficient to cause steric repulsion between the fungal macromolecules and the AFM tip, but this repulsion does not prevent the cells from adhering strongly to silicon nitride or from attaching to quartz media. In the AFM experiment, steric repulsion is forcibly overcome, since the tip is moved into contact with the fungal surface. In the column transport experiment, it appears that hydrodynamics can provide sufficient force to allow the fungal cells to contact the quartz collectors, even in the presence of steric repulsion caused by exterior macromolecules.

By later in the exponential phase, the uronic acid polymers have increased in their density, and a large population of pullulan molecules has also appeared. In terms of total polymer population, the uronic acid polymers make up only ~10%, with pullulan accounting for the remainder. These LEP cells possess both the short uronic acid based polymers

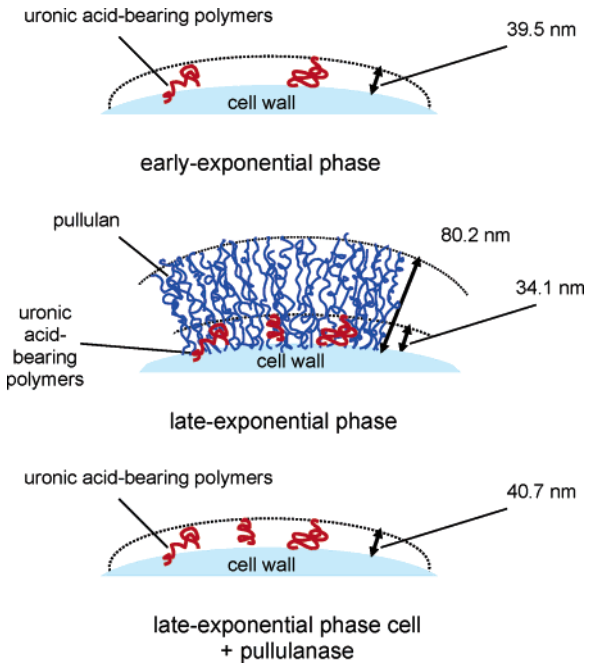

Figure 7. Schematic representation of macromolecules on exterior of *A. pullulans*, under the conditions examined in this study.

(34.1 nm) and the longer pullulan molecules (80.2 nm). Stericrepulsion is increased, and both the adhesion (between the fungus and silicon nitride) and attachment (between the fungus and quartz) are decreased.

Interestingly, the LEP + pullulanase cells behave in a way that is similar to the LEP cells in terms of adhesion and attachment. Treatment with pullulanase removed the second subpopulation of molecules, and the polymer lengths were again short and representative of the uronic acid-based molecules (40.7 nm). Although the steric repulsion (shown via AFM approach curves) is much decreased between LEP and LEP + pullulanase cells due to the removal of the large pullulan molecules, the adhesion forces from retraction data are almost the same and the attachment to quartz is nearly the same. If steric interactions alone could explain fungal adhesion and attachment, then we would have expected the LEP cells treated with pullulanase to attach less and show lower adhesion forces than those cells with intact pullulan.

These results suggest that measures and predictions of steric repulsion from AFM experiments need to be treated cautiously, since steric repulsions are almost always observed in AFM approach measurements on bacteria and fungi. During approach cycles in water or buffer (with various probes or as cell probes with varying substrates), *Pseudomonas putida* KT2442,[25,26] *Pseudomonas aeruginosa*,[36] *Burkholderia cepacia* G4,[25] several strains of *Escherichia coli*,[37,49,50] spores of *Aspergillus oryzae*,[51] *Saccharomyces cerevisiae* (with COOH or OH terminated probes),[52] nine different strains of the oral bacterium *Streptococcus mitis*,[53] and the isolated extracellular polymeric material (EPS) from *Pseudomonas atlantica*[54] showed only repulsion. Rarely, attractive interactions have been observed, such as with *Candida parapsilosis* and glass,[36] with *Bacillus mycoides* spores and hydrophobically treated glass,[55] and glutaraldehyde-treated *E. coli* cells interacting with mica, glass, Teflon, or polystyrene.[56] The sources of the attractions are believed to be specific interactions between microbial macromolecules and the interacting substrate. Although such interactions would hypothetically be present in all cases, often steric repulsion is so large that it masks all such specific interactions. Due to the widespread appearance of steric interactions in AFM approach curves on fungal and bacterial cells, it is often more useful to analyze retraction curve data to describe adhesion and attachment phenomena.

Effect of Physiological Status on Biopolymer Production and Adhesion/Attachment Behavior. The adhesion of fungi, such as *A. pullulans*, to various surfaces including soil, plants, and human tissue, depends in large part on the polysaccharides or other biomacromolecules produced by the microorganism. The physiological status of the microbe and given environmental conditions determines which macromolecules are produced and excreted, and these macromolecules influence surface adhesion or attachment.

The biosynthesis of pullulan by *A. pullulans* has been widely studied, but many contradictory results are found in the literature since several factors affect polymer production. Strain variability plays an important role in determining how biosynthesis proceeds, and factors such as carbon source, cell morphology, oxygen concentration, temperature, shear stress (i.e., in a fermentor), and trace amounts of vitamins and minerals all affect pullulan production.[1]

Some studies have shown that pullulan is produced more in stationary, compared to exponential-phase, growth.[6,57] This is consistent with the idea that pullulan is a secondary metabolite, and so it is produced only when growth decreases, although by a strict definition, secondary metabolites refer to diffusible products, and thus pullulan would not be such a compound. Other studies have shown that pullulan production is optimal during active cell growth[58] or that synthesis is independent of biomass/growth.[59] In our study, adhesion was greater in the earlier growth phase. We could suppose that it is advantageous for the microbe to adhere in order to gain nutrients or to seek protection from predators in the aqueous suspension, but these ideas are very speculative at this time.

If we look to the literature for other examples of the relationship between physiologic status and adhesion, we find varied relationships between metabolic activity and microbial adhesion or interaction forces. For example, dormant versus activated fungal spores have exhibited different adhesion behavior and elastic properties in AFM measurements.[51,60] A relationship between growth phase and physiological status was also observed for *Saccharomyces cerevisiae*. The stationary phase cells adhered most strongly to mica, and this increased adhesion was correlated with an increased hydrophobicity and lower zeta potential than cells harvested from either exponential or death phases.[61]

Conclusions

The adhesion of the microfungus *A. pullulans* was studied via AFM and column transport experiments. Adhesion forces to silicon nitride were correlated with retention on quartz porous media. The adhesion forces of the microbe could be related to the nature of its cell surface macromolecules, which

depended on the microbe's growth phase. EEP cells were characterized by high adhesion for the AFM tip, high retention to quartz media, and a small polymer brush layer (39.5 nm) that was composed of uronic acid bearing polymers. LEP cells showed two subpopulations of polymer molecules, both short (34.1 nm; 10% of molecules) uronic acid polymers and long (80.2 nm) chains of pullulan. LEP cells demonstrated increased steric repulsion with the silicon nitride AFM tips, due to the appearance of the larger pullulan molecules and due to an increase in the density of the uronic acid polymers. When the enzyme pullulanase was applied to LEP cells, only a single population of polymer molecules was detected, with an equilibrium polymer length of 40.7 nm. Pullulanase-treatment had a minimal effect on the collision efficiency of LEP cells or on the average adhesion force (with silicon nitride) from AFM experiments, suggesting that a molecule other than pullulan was responsible for the adhesion and attachment of LEP cells to silicon nitride and quartz. Our results suggest that steric interactions alone do not dictate whether fungal cells will attach to a given surface.

These results emphasize that (1) the adhesion of *A. pullulans* is related to the presence and physicochemical properties of specific cell surface macromolecules, which depend on physiologic status; (2) AFM retraction measurements, which give adhesion forces, are better predictors of microbial attachment than are predictions of steric interactions from AFM approach curves; and (3) a modified van der Waals model, which accounts for surface roughness, is better able to characterize the adhesive interactions between a microbe and a model surface than the conventional van der Waals model. In the future, further experiments could be done to extend these experiments toward environmental conditions, such as by characterizing the bacteria at higher ionic strengths.

Acknowledgment. This publication was made possible in part by a grant from the National Science Foundation (BES-0238627). We also acknowledge the donors of the Petroleum Research Fund of the American Chemical Society, for partial support of this work (PRF 38988-G2). In addition, J.M.P. was funded by an Academic Excellence Award from the GE Fund at the Pennsylvania State University, through the Women in Engineering Program. We are grateful to Ms. Barbara Bogue for her assistance with this award. We appreciate the assistance of Prof. George Pins for allowing us use of his optical microscope, Dr. Nehal Abu-Lail, for her comments on a previous version of the manuscript, and Mr. Ray Emerson, for creating an Excel macro to analyze the AFM data. The anonymous reviewers are also thanked for their assistance, which greatly improved this manuscript.

References and Notes

(1) Leathers, T. D. Pullulan. In *Polysaccharides II*; Steinbuchel, A., Ed.; Wiley VCH: New York, 2002; p 1.
(2) Chabasse, D. *J. Mycol. Med.* **2002**, *12*, 65.
(3) Salkin, I. F.; Martinez, J. A.; Kemna, M. E. *J. Clin. Microbiol.* **1986**, *23*, 828.
(4) Clark, E. C.; Silver, S. M.; Hollick, G. E.; Rinaldi, M. G. *Am. J. Nephrol.* **1995**, *15*, 353.
(5) Pollock, T. J.; Thorne, L.; Armentrout, R. W. *Appl. Environ. Microbiol.* **1992**, *58*, 877.
(6) Leathers, T. D.; Nofsinger, G. W.; Kurtzman, C. P.; Bothast, R. J. *J. Ind. Microbiol.* **1988**, *3*, 231.
(7) Bouveng, H. O.; Kiessling, H.; Lindberg, B.; McKay, J. *Acta Chem. Scand.* **1962**, *17*, 615.
(8) Bouveng, H. O. *Acta Chem. Scand.* **1963**, *17*, 1351.
(9) Gibson, L. H.; Coughlin, R. W. *Biotechnol. Prog.* **2002**, *18*, 675.
(10) Catley, B. J.; Hutchison, A. *Trans. Br. Mycol. Soc.* **1981**, *76*, 451.
(11) Taguchi, R.; Sakano, Y.; Kikuchi, Y.; Sakuma, M.; Kobayashi, T. *Agric. Biol. Chem.* **1973**, *37*, 1635.
(12) Catley, B. J.; McDowell, W. *Carbohydr. Res.* **1982**, *153*, 79.
(13) Isralides, C.; Smith, A.; Scanlon, B.; Barnett, C. *Biotechnol. Genet. Eng. Rev.* **1999**, *16*, 309.
(14) Andrews, J. H.; Harris, R. F.; Spear, R. N.; Lau, G. W.; Nordheim, E. V. *Can. J. Microbiol.* **1994**, *40*, 6.
(15) Bardage, S. L.; Bjurman, J. *Can. J. Microbiol.* **1998**, *44*, 954.
(16) Dufrêne, Y. F. *Nat. Rev. Microbiol.* **2004**, *2*, 451.
(17) Bowen, W. R.; Lovitt, R. W.; Wright, C. J. *J. Coll. Interface Sci.* **2000**, *228*, 428.
(18) Gallardo-Moreno, A. M.; Méndez-Vilas, A.; González-Martín, M. L.; Nuevo, M. J.; Bruque, J. M.; Garduño, E.; Pérez-Giraldo, C. *Langmuir* **2002**, *18*, 3639.
(19) Hobbie, J. E.; Daley, R. J.; Jasper, S. *Appl. Environ. Microbiol.* **1977**, *59*, 2746.
(20) Lee, J. W.; Yeomans, W. G.; Allen, A. L.; Deng, F.; Gross, R. A.; Kaplan, D. L. *Appl. Environ. Microbiol.* **1999**, *65*, 5265.
(21) Galambos, J. T. *Anal. Biochem.* **1967**, *19*, 119.
(22) Blumenkrantz, N.; Asboe-Hansen, G. *Anal. Biochem.* **1973**, *54*, 484.
(23) Filisetti-Cozzi, T. M. C. C.; Carpita, N. C. *Anal. Biochem.* **1991**, *197*, 157.
(24) Gerhardt, P., Murray, R. G. E., Wood, W. A., Krieg, N. R., Eds.; *Methods for General and Molecular Bacteriology*; American Society for Microbiology: Washington, DC, 1994.
(25) Camesano, T. A.; Logan, B. E. *Environ. Sci. Technol.* **2000**, *34*, 3354.
(26) Abu-Lail, N. I.; Camesano, T. A. *Biomacromolecules* **2003**, *4*, 1000.
(27) Camesano, T. A.; Logan, B. E. *Langmuir* **2000**, *16*, 4563.
(28) Cleveland, J. P.; Manne, S.; Bocek, D.; Hansma, P. K. *Rev. Sci. Instrum.* **1993**, *64*, 403.
(29) Tomitori, M.; Arai, T. *Appl. Surf. Sci.* **1999**, *140*, 432.
(30) Ducker, W. A.; Senden, T. J.; Pashley, R. M. *Langmuir* **1992**, *8*, 1831.
(31) Alexander, S. *J. Phys. II (Paris)* **1977**, *38*, 983.
(32) de Gennes, P. G. *Adv. Colloid Interface Sci.* **1987**, *27*, 189.
(33) Butt, H.-J.; Kappl, M.; Mueller, H.; Raiteri, R. *Langmuir* **1999**, *15*, 2559.
(34) Drummond, C. J.; Senden, T. J. *Colloids Surf. A: Physicochem. Eng. Aspects* **1994**, *87*, 217.
(35) Senden, T. J.; Drummond, C. J. *Colloids Surf. A: Physicochem. Eng. Aspects* **1995**, *94*, 29.
(36) Emerson, R. J.; Camesano, T. A. *Appl. Environmen. Microbiol.* **2004**, *70*, 6012.
(37) Abu-Lail, N. I.; Camesano, T. A. *Environmen. Sci. Technol.* **2003**, *37*, 2173.
(38) Lahlou, M. H., H.; Sprinael, D.; Ortega-Calvo, J.-J. *Environmen. Sci. Technol.* **2000**, *34*, 3649.
(39) Yao, K.-M.; Habibian, M. T.; O'Melia, C. R. *Environ. Sci. Technol.* **1971**, *5*, 1105.
(40) Logan, B. E.; Jewett, D. G.; Arnold, R. G.; Bouwer, E. J.; O'Melia, C. R. *J. Environmen. Eng.* **1995**, *121*, 869.
(41) Rajagopalan, R.; Tien, C. *AIChE J.* **1976**, *22*, 523.
(42) Bell, C. H.; Arora, B. S.; Camesano, T. A. Submitted for publication.
(43) Gad, M.; Itoh, A.; Ikai, A. *Cell Biol. Int.* **1997**, *21*, 697.
(44) Logan, B. E. *Environmental Transport Processes*; John Wiley & Sons: New York, 1999.
(45) Johnson, P. R. *J. Colloid Interface Sci.* **1999**, *209*, 264.
(46) Zhmud, B. V.; Sonnefeld, J.; Bergstrom, L. *Colloids Surf. A: Physicochem. Eng. Aspects* **1999**, *158*, 327.
(47) Rabinovich, Y. I.; Adler, J. J.; Ata, A.; Singh, R. K.; Moudgil, B. M. *J. Colloid Interface Sci.* **2000**, *232*, 10.
(48) Rabinovich, Y. I.; Adler, J. J.; Ata, A.; Singh, R. K.; Moudgil, B. M. *J. Colloid Interface Sci.* **2000**, *232*, 17.
(49) Burks, G. A.; Velegol, S. B.; Paramanova, E.; Lindenmuth, B. E.; Feick, J. D.; Logan, B. E. *Langmuir* **2003**, *19*, 2366.
(50) Velegol, S. B.; Logan, B. E. *Langmuir* **2002**, *18*, 5256.
(51) Van der Aa, B. C.; Asther, M.; Dufrêne, Y. F. *Colloid Surf. B: Biointerfaces* **2002**, *24*, 277.
(52) Ahimou, F.; Denis, F. A.; Touhami, A.; Dufrêne, Y. F. *Langmuir* **2002**, *18*, 9937.
(53) Vadillo-Rodriguez, V.; Busscher, H. J.; Norde, W.; de Vries, J.; van der Mei, H. C. *Langmuir* **2003**, *19*, 2372.

(54) Frank, B. P.; Belfort, G. *Langmuir* **1997**, *13*, 6234.
(55) Bowen, W. R.; Fenton, A. S.; Lovitt, R. W.; Wright, C. J. *Biotechnol. Bioeng.* **2002**, *79*, 170.
(56) Ong, Y.-L.; Razatos, A.; Georgiou, G.; Sharma, M. M. *Langmuir* **1999**, *15*, 2719.
(57) Ueda, S.; Fujita, K.; Komatsu, K.; Nakashima, Z. *Appl. Microbiol.* **1963**, *11*, 211.
(58) Klimek, J.; Ollis, D. F. *Biotechnol. Bioeng.* **1980**, *22*, 2321.
(59) Augustin, J.; Kuniak, L.; Hudecova, D. *Biol., Bratislava* **1997**, *52*, 399.
(60) Dufrêne, Y. F.; Boonaert, C. J. P.; van der Mei, H. C.; Busscher, H. J.; Rouxhet, P. G. *Ultramicroscopy* **2001**, *86*, 113.
(61) Bowen, W. R.; Lovitt, R. W.; Wright, C. J. *J. Colloid Interface Sci.* **2001**, *237*, 54.

BM0492935